

Variations in earthquake-size distribution across different stress regimes

Danijel Schorlemmer¹, Stefan Wiemer¹ & Max Wyss²

The earthquake size distribution follows, in most instances, a power law^{1,2}, with the slope of this power law, the 'b value', commonly used to describe the relative occurrence of large and small events (a high b value indicates a larger proportion of small earthquakes, and vice versa). Statistically significant variations of b values have been measured in laboratory experiments, mines and various tectonic regimes such as subducting slabs, near magma chambers, along fault zones and in aftershock zones³. However, it has remained uncertain whether these differences are due to differing stress regimes, as it was questionable that samples in small volumes (such as in laboratory specimens, mines and the shallow Earth's crust) are representative of earthquakes in general. Given the lack of physical understanding of these differences, the observation that b values approach the constant 1 if large volumes are sampled⁴ was interpreted to indicate that $b = 1$ is a universal constant for earthquakes in general⁵. Here we show that the b value varies systematically for different styles of faulting. We find that normal faulting events have the highest b values, thrust events the lowest and strike-slip events intermediate values. Given that thrust faults tend to be under higher stress than normal faults we infer that the b value acts as a stress meter that depends inversely on differential stress.

To resolve the issue of influence of stress on b, we search several high-quality large data sets, including a global one, for systematic dependence of b on the style of faulting. To estimate b values, we use the maximum-likelihood method⁶, with uncertainties estimated as described in ref. 7. We require at least 100 events per sample for computations of b, but mark all b values that are computed from less than 200 events. For consistency in the analysis we binned magnitudes in all catalogues to $\Delta M = 0.1$. In addition, we selected periods of homogeneous recording, determined their overall magnitude of completeness M_c for each catalogue and cut the catalogues accordingly (Table 1). The source depths were restricted to 50 km, because deep events may obey different laws of faulting. The significance of differences between b values is computed with the Utsu-test⁸ as the probability P_b that the b values are not different. Values of $\log P_b \leq -1.3$ and $\log P_b \leq -1.9$ indicate significant and highly significant differences, respectively.

Earthquake focal mechanisms are now determined routinely for thousands of events. For this study we use the best sources of focal mechanisms available worldwide: the global Harvard CMT moment tensor catalogue, a catalogue of relocated events of southern California (SCSN)⁹, a northern California data set (NCSN), a data set of events from the Kanto-Tokai region of Japan, and the F-Net data for all of Japan. From the Kanto-Tokai catalogue we excluded volcanic and geothermal areas (140.30° E, 36.99° N; 137.73° E, 35.71° N; 136.78° E, 35.74° N; 136.64° E, 35.25° N; 137.01° E, 34.58° N; 138.54° E, 34.58° N; 139.00° E, 34.78° N; 138.94° E, 35.34° N;

139.03° E, 35.34° N; 139.46° E, 34.82° N; 140.05° E, 34.91° N; 140.90° E, 35.69° N; 141.36° E, 36.57° N; 141.37° E, 36.72° N; 140.55° E, 36.98° N; 140.30° E, 36.99° N).

Two quality descriptors in the Californian catalogues (one in the NEID Kanto-Tokai catalogue, namely misfit) were used to limit the analysis to the high-quality events: solution misfit ≤ 0.2 and station distribution ratio ≥ 0.5 .

For classifying events as strike-slip, thrust or normal events, we use the rake angle λ within a given range of $\pm\gamma$ (Aki-Richards convention: $\lambda = 0$ or $\lambda = \pm 180^\circ$ as strike-slip, $\lambda = 90^\circ$ as thrust, and $\lambda = -90^\circ$ as normal events). Because the Californian catalogues contain only one nodal plane, we computed the corresponding second planes.

We performed two different computations. First, we computed b values as a function of the rake angles λ of the single planes with a constant range γ (b_λ plot). We used $\gamma = 20^\circ$ for the SCSN data, $\gamma = 60^\circ$ for the NEID F-Net data, and $\gamma = 40^\circ$ for the other catalogues. The different ranges were used to smooth the results according to the amount of available data. Second, to explore the separation of b values into different classes, we computed b values as a function of the range γ for all three classes of events (b_γ plot). Hereby, the γ value was varied from 175° to 5° in steps of -10° , and both rake angles λ of the two nodal planes had to fall within the given range. For $\gamma \geq 45^\circ$, events may fall into two or more classes.

We computed the b_λ plot for the SCSN data (Fig. 1a). This catalogue is probably the highest-quality regional data set of focal mechanisms available worldwide, because of the high density of stations, the relocation of events and recomputation of take-off angles with a three-dimensional velocity model. These data show that the differences in b values for the three classes of events are larger than the errors of individual samples and are significant (Table 2). Normal events (green) show the highest b values ($b_{NR} \approx 1.1$), strike-slip events (red) show intermediate values ($b_{SS} \approx 0.9$) and thrust events (blue) the lowest ($b_{TH} \approx 0.7$). The transition between the average b value and the extreme b values (normal, thrust) is pronounced.

In the b_γ plot of the SCSN data (Fig. 1b), one can see that with smaller γ , b values of normal and thrust events start to deviate

Table 1 | Selection parameters of the catalogues

Network	Period	M_c	Depth (km)	No. of events
Harvard CMT	1.1.1980-31.12.2004	5.5	0-50	7,636
SCSN	1.1.1981-31.12.2003	2.5	all	14,003
NCSN	1.1.1981-31.12.2004	3.0	all	4,250
NEID F-Net	4.1.1997-31.12.2004	4.5	0-50	1,579
NEID Kanto-Tokai	1.1.1982-1.7.2003	3.0	0-50	2,337

¹Swiss Seismological Service, ETH Zürich, ETH Hönggerberg, Schafmattstr. 30, 8093 Zürich, Switzerland. ²World Agency of Planetary Monitoring and Earthquake Risk Reduction, Route de Jargonnant 2, 1207 Genève, Switzerland.

systematically from the regional average and reach their extreme for pure event classes with range $\gamma \leq 5^\circ$. Strike-slip events show only minor deviation from the regional average b value, regardless of the range γ . Only for $\gamma = 5^\circ$ is the b value significantly higher than the average. The differences in the frequency–magnitude distribution between pure thrust and pure normal events are statistically highly significant (Fig. 1c and Table 2).

The b -value variations of the Harvard catalogue are less pronounced; however, they show the same dependence on faulting style (Fig. 1d, e). The separation is clearer when using only the first nodal plane for classifying events (Fig. 1e, inset) rather than both nodal planes (Fig. 1e). Although each catalogue covers a different range of magnitudes, the frequency–magnitude distributions emphasize the similarity of the b values for the two displayed classes of events (Fig. 1c).

The data in all three additional catalogues show essentially the same systematic dependence of b on faulting style (Fig. 2). The absolute level of b does not concern us here, because it can vary in different regions and for different networks. The important observation is that, in all cases, normal events have the highest b values, followed by strike-slip and thrust events. In some data sets the separation is no longer clear for the narrowest ranges γ of λ because the error bars increase as a result of small sample sizes.

The data sets analysed are very different in depth distribution, magnitude range and tectonic environment. Nevertheless, all data sets show the same dependence of b on focal mechanisms.

The uniformity of the separation of b values according to faulting type in these tectonically different data sets requires a universal interpretation. We propose that the differential stress, and indirectly the confining pressure (to which the differential stress is tied), is the parameter most strongly controlling faulting types, thus influencing differences in b . This inverse relationship follows because we show that $b_{\text{TH}} < b_{\text{SS}} < b_{\text{NR}}$, and it is known that for a given vertical stress σ_v the mean stresses obey the relationship $\bar{\sigma}_{\text{TH}} > \bar{\sigma}_{\text{SS}} > \bar{\sigma}_{\text{NR}}$.

Our results imply that the inverse relationship between differential stress $\Delta\sigma$ and b is universally valid, spanning the range from submillimetres to hundreds of kilometres of rupture length. The b value can therefore be interpreted as a ‘stressmeter’ in the Earth’s crust. However, locally, secondary effects can come from material properties^{10,11} and from modifications of the stress tensor by pore pressure¹².

The idea that depths might be the controlling factor, in general, can be ruled out because the average depths of the three classes of events are not systematically ordered according to the b values. Depth is also not a good candidate to be a universal factor controlling b , because the trends reported are opposite in California^{13,14} and Japan¹⁵. The degree of material heterogeneity¹⁰ as a fundamental cause of these universal differences can also be ruled out, because the observation is valid for small as well as larger earthquakes and for all existing tectonic settings.

Previous studies^{4,16} based on fewer data and a less quantitative analysis of focal mechanism reported that the size distribution β of moments in the Harvard CMT catalogue (0–70 km depth) obey the relationship $\beta_{\text{NR}} > \beta_{\text{TH}} > \beta_{\text{SS}}$. However, the most comparable computation of Kagan, using the entire catalogue in the period 1987–1999 with a completeness of $M_c = 5.4$ reproduces the relation that we found: $(\beta_{\text{NR}} = 0.731) > (\beta_{\text{SS}} = 0.643) > (\beta_{\text{TH}} = 0.642)$.

The inverse relationship between stress and b is consistent with a range of other observations: laboratory rock specimens^{11,17}, mines¹⁸ and increased pore pressure^{12,19} (which decreases the differential stress). For the Los Angeles Basin, it was found²⁰ that $b_{\text{SS}} = 1.1$ and $b_{\text{TH}} = 0.7$ for strike-slip and thrust events, respectively. Although this result was based on only 144 and 78 earthquakes, respectively, it supports our findings. Finally, the strong differences in b between locked parts of faults, where b values are low, and creeping sections with much higher b (refs 21–23), are consistent with the model. The shear strength is assumed to be higher in a locked section than in creeping sections. This results in high $\Delta\sigma$ and low b values for

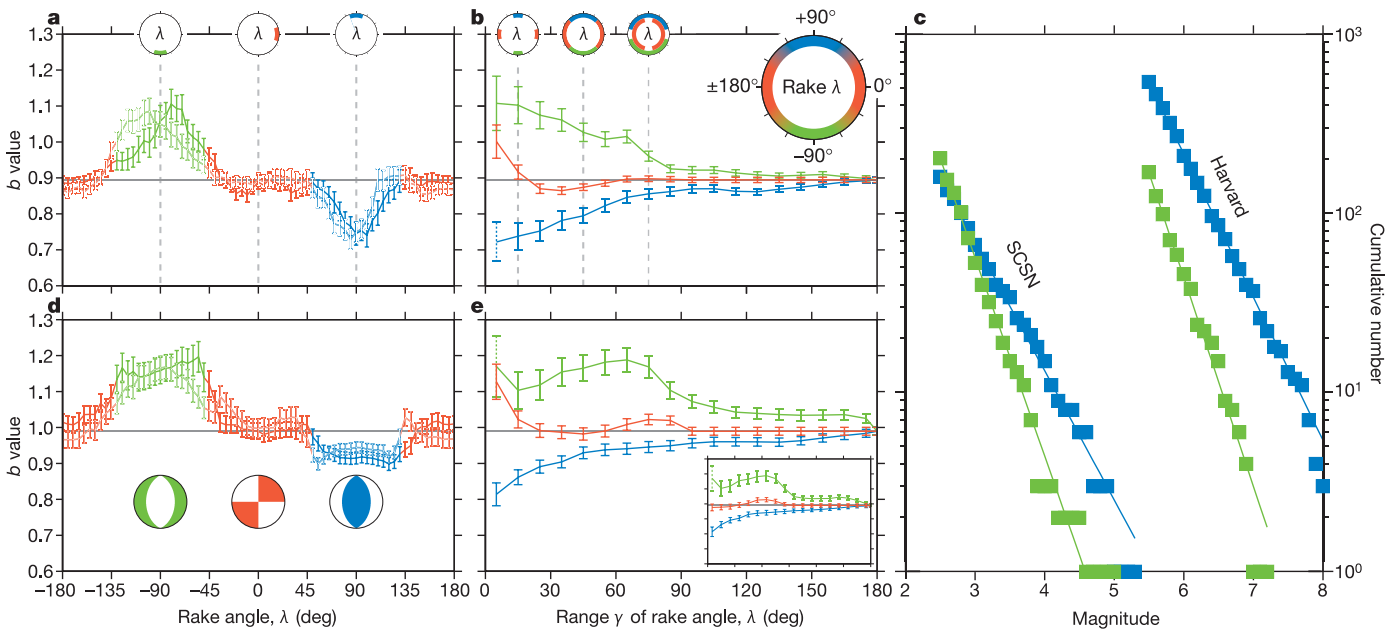


Figure 1 | Plots of b against rake angle and range of rake angle. **a**, b_λ plot of events in southern California, from the SCSN catalogue. In all frames the green, red and blue lines (solid, first plane; outlined, second plane) mark the b values of mainly normal, strike-slip and thrust events, respectively; the grey line marks the average b value and the vertical bars indicate the standard error⁷. (Solid bars are used for samples with $N \geq 200$, and dashed bars for samples with $200 > N \geq 100$). The circles at the top of the frame show the rake λ used for computing the b values $\lambda = -90^\circ \pm \gamma$, $\lambda = 0^\circ \pm \gamma$

and $\lambda = 90^\circ \pm \gamma$, $\gamma = 20^\circ$. **b**, b_γ plot of events in southern California. The circles at the top of the frame show the range of rake λ used for computing the b values ($\gamma = 15^\circ, 45^\circ$ and 75°). Inset, circle explaining the rake values and the corresponding colours of the classes of events. **c**, Frequency–magnitude distributions for pure normal (green) and pure thrust (blue) events of the SCSN and Harvard catalogues ($\gamma = 5^\circ$). **d**, As **a** for the Harvard catalogue. **e**, As **b** for the Harvard catalogue. Inset, as main panel but considering only the rake of the first nodal plane.

Table 2 | Values of b for three different ranges γ of the three classes of events and their Utsu-test probabilities ($\log P_b$) of being different

Network	Range γ (deg)	b_{TH}	b_{SS}	b_{NR}	$\log P_b$ TH-SS	$\log P_b$ SS-NR	$\log P_b$ TH-NR
SCSN	05	0.72 ± 0.05	1.00 ± 0.05	1.11 ± 0.08	-2.83	-0.30	-3.61
	25	0.75 ± 0.03	0.87 ± 0.01	1.07 ± 0.04	-2.52	-5.95	-9.49
	45	0.79 ± 0.02	0.87 ± 0.01	1.03 ± 0.03	-2.32	-7.17	-10.38
Harvard	05	0.81 ± 0.03	1.13 ± 0.05	1.17 ± 0.08	-5.19	-0.04	-3.67
	25	0.89 ± 0.02	0.99 ± 0.02	1.12 ± 0.04	-2.67	-1.55	-5.52
	45	0.93 ± 0.02	0.98 ± 0.02	1.17 ± 0.04	-0.94	-4.51	-8.07
NCSN	05	-	-	-	-	-	-
	25	0.67 ± 0.05	0.81 ± 0.02	1.01 ± 0.06	-1.14	-1.99	-3.61
	45	0.73 ± 0.04	0.91 ± 0.02	1.00 ± 0.04	-3.50	-0.74	-4.52
Kanto-Tokai	05	-	-	-	-	-	-
	25	0.68 ± 0.03	0.89 ± 0.05	1.03 ± 0.09	-2.72	-0.35	-2.78
	45	0.66 ± 0.02	0.90 ± 0.04	1.06 ± 0.07	-7.50	-0.79	-6.44
F-Net	05	-	-	-	-	-	-
	25	0.80 ± 0.04	1.02 ± 0.07	1.06 ± 0.08	-1.50	-0.02	-1.84
	45	0.78 ± 0.03	1.09 ± 0.05	1.05 ± 0.05	-5.28	-0.05	-3.57

Significant $\log P_b$ values are bold.

locked sections, whereas creeping sections exhibit low $\Delta\sigma$ and high b values. This conceptual model relating b to fault locking was recently tested and supported by the magnitude 6.0 Parkfield, California, event in 2004 (ref. 24), which almost exclusively ruptured areas of the San Andreas fault previously mapped as regions of low b .

The physical model offered by Scholz¹¹ as an explanation for the stress dependence of b emphasizes the role of differential stress. He argues that in a rock mass with varying resistance to faulting (and varying stress concentration) a rupture is likely to connect one high-stress subvolume to the next, because the system contains more

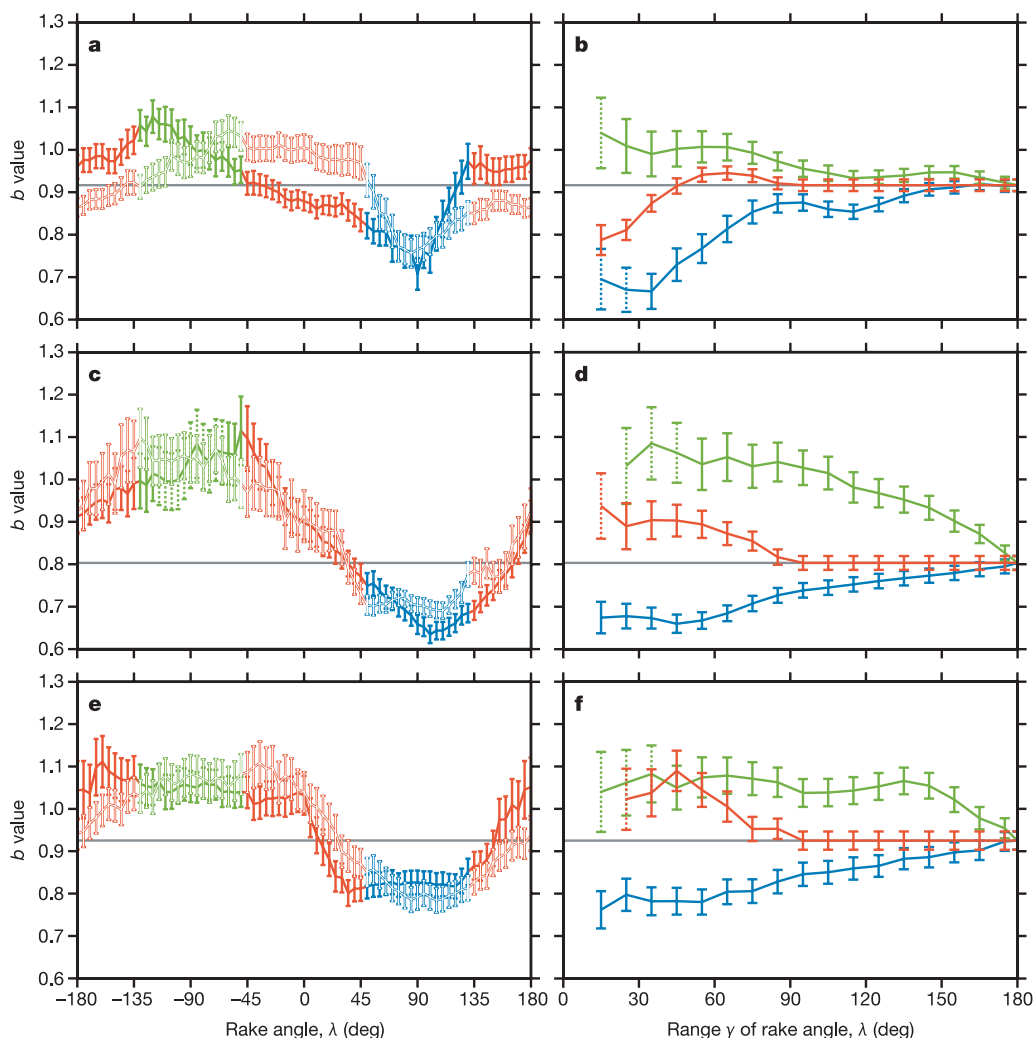


Figure 2 | b_λ plots and b_γ plots for the NCSN catalogue (a, b), the NEID Kanto-Tokai catalogue (c, d) and the NEID F-Net catalogue (e, f). In all frames the green, red and blue lines (solid, first plane; outlined, second plane) mark the b values of mainly normal, strike-slip and thrust events,

respectively; the grey line marks the average b value and the vertical bars indicate the standard error⁷. (Solid bars are used for samples with $N \geq 200$, dashed bars for samples with $200 > N \geq 100$).

energy. Thus, earthquakes grow larger in a high-stress environment. This finding is additionally supported by fractal simulations²⁵. Amitrano¹⁷ proposed a more geometrical model, emphasizing the role of confining pressure. On the basis of a numerical model, he argued that, at low confining pressure, the internal friction angle is such that failure in a given element can influence other elements only in restricted directions. At high confining pressure, the angle of internal friction decreases and interactions with elements containing defects are possible in all directions. Thus, failures grow larger in a system under high confining pressure.

The dependence of b on differential stress suggests that a systematic decrease in b towards the end of the seismic cycle^{26,27} could indeed exist. However, the amplitude of the differential stress increase during the loading cycle is probably an order of magnitude smaller than in laboratory experiments and in mines. The high-quality data sets necessary to test this hypothesis are probably not yet available.

One of the implications of the universal dependence of b on differential stress is that earthquake hazard analysis should be rethought. The b value is a critical parameter in studies of seismic hazard. If events of different faulting styles within one seismogenic zone follow different recurrence laws, and because faulting styles influence ground motions²⁸, estimating the recurrence for each faulting style separately may produce more accurate estimates of seismic hazard. In addition, hazard studies should pay attention to spatial heterogeneity in b values, because it is directly related to the distribution of differential stresses in the Earth's crust.

Received 1 February; accepted 2 August 2005.

- Ishimoto, M. & Iida, K. Observations of earthquakes registered with the microseismograph constructed recently. *Bull. Earthquake Res. Inst. Tokyo Univ.* **17**, 443–478 (1939).
- Gutenberg, B. & Richter, C. F. Frequency of earthquakes in California. *Bull. Seismol. Soc. Am.* **34**, 185–188 (1944).
- Wiemer, S. & Wyss, M. Mapping spatial variability of the frequency–magnitude distribution of earthquakes. *Adv. Geophys.* **45**, 259–302 (2002).
- Frohlich, C. & Davis, S. D. Teleseismic b values; or, much ado about 1.0. *J. Geophys. Res.* **98**, 631–644 (1993).
- Kagan, Y. Y. Universality of the seismic moment–frequency relation. *Pure Appl. Geophys.* **155**, 537–574 (1999).
- Bender, B. Maximum likelihood estimation of b values for magnitude grouped data. *Bull. Seismol. Soc. Am.* **73**, 831–851 (1983).
- Shi, Y. & Bolt, B. A. The standard error of the magnitude–frequency b -value. *Bull. Seismol. Soc. Am.* **72**, 1677–1687 (1982).
- Utsu, T. *Report of the Joint Research Institute for Statistical Mathematics* Vol. 34, 139–157 (Institute for Statistical Mathematics, Tokyo, 1992).
- Hauksson, E. Crustal structure and seismicity distribution adjacent to the Pacific and North America plate boundary in southern California. *J. Geophys. Res.* **105**, 13875–13903 (2000).
- Mogi, K. Magnitude–frequency relations for elastic shocks accompanying fractures of various materials and some related problems in earthquakes. *Bull. Earthquake Res. Inst. Univ. Tokyo* **40**, 831–853 (1962).
- Scholz, C. H. The frequency–magnitude relation of microfracturing in rock and its relation to earthquakes. *Bull. Seismol. Soc. Am.* **58**, 399–415 (1968).
- Wyss, M. Towards a physical understanding of the earthquake frequency distribution. *Geophys. J. R. Astron. Soc.* **31**, 341–359 (1973).
- Mori, J. & Abercrombie, R. E. Depth dependence of earthquake frequency–magnitude distributions in California: Implications for rupture initiation. *J. Geophys. Res.* **102**, 15081–15090 (1997).
- Gerstenberger, M., Wiemer, S. & Giardini, D. A systematic test of the hypothesis that the b value varies with depth in California. *Geophys. Res. Lett.* **28**, 57–60 (2001).
- Wyss, M. & Matsumura, S. Most likely locations of large earthquakes in the Kanto and Tokai areas, Japan, based on the local recurrence times. *Physics of the Earth and Planetary Interiors* **131**, 173–184 (2002).
- Kagan, Y. Y. Seismic moment distribution revisited: I. Statistical results. *Geophys. J. Int.* **148**, 520–541 (2002).
- Amitrano, D. Brittle–ductile transition and associated seismicity: Experimental and numerical studies and relationship with the b value. *J. Geophys. Res.*, B2044 (2003) (doi:10.1029/2001JB000680).
- Urbancic, T. I., Trifu, C. I., Long, J. M. & Young, R. P. Space-time correlations of b -values with stress release. *Pure Appl. Geophys.* **139**, 449–462 (1992).
- Wiemer, S., McNutt, S. R. & Wyss, M. Temporal and three-dimensional spatial analysis of the frequency–magnitude distribution near Long Valley caldera, California. *Geophys. J. Int.* **134**, 409–421 (1998).
- Hauksson, E. Earthquakes, faulting, and stress in the Los Angeles basin. *J. Geophys. Res.* **95**, 15365–15394 (1990).
- Amelung, F. & King, G. The difference between earthquake scaling laws for creeping and non-creeping faults. *Geophys. Res. Lett.* **24**, 507–510 (1997).
- Wiemer, S. & Wyss, M. Mapping the frequency–magnitude distribution in asperities: An improved technique to calculate recurrence times? *J. Geophys. Res.* **102**, 15115–15128 (1997).
- Schorlemmer, D., Wiemer, S. & Wyss, M. Earthquake statistics at Parkfield: 1. Stationarity of b -values. *J. Geophys. Res.* **109**, B12307 (2004) (doi:10.1029/2004JB003234).
- Schorlemmer, D. & Wiemer, S. Microseismicity data forecast rupture area. *Nature* **434**, 1086 (2005).
- Huang, J. & Turcotte, D. L. Fractal distributions of stress and strength and variations of b -value. *Earth Planet. Sci. Lett.* **91**, 223–230 (1988).
- Smith, W. D. The b -values as an earthquake precursor. *Nature* **289**, 136–139 (1981).
- Lei, X. *et al.* Detailed analysis of acoustic emission activity during catastrophic fracture of faults in rock. *J. Struct. Geol.* **26**, 247–258 (2004).
- Oglesby, D. D., Archuleta, R. J. & Nielsen, S. B. Dynamics of dip-slip faulting: Explorations in two dimensions. *J. Geophys. Res.* **105**, 13643–13653 (2000).

Acknowledgements We thank E. Hauksson, D. Giardini, M. Mai, M. Gerstenberger, D. Jackson, J. Woessner and G. Hillers for discussions. We thank the Northern California Seismic Network, US Geological Survey, Menlo Park, and the Berkeley Seismological Laboratory, University of California, Berkeley, for the catalogue including phase data, and the National Research Institute for Earth Science and Disaster Prevention for mechanism solutions of the Kanto-Tokai area.

Author Information Reprints and permissions information is available at npg.nature.com/reprintsandpermissions. The authors declare no competing financial interests. Correspondence and requests for materials should be addressed to D.S. (daniel@sed.ethz.ch).